Variable-Density Radial View-Ordering and Sampling for Time-Optimized 3D Cartesian Imaging

Joseph Y. Cheng[1], Tao Zhang[1], Marcus T. Alley[2], Michael Lustig[3], Shreyas S. Vasanawala[2], John M. Pauly[1]

[1]*Electrical Engineering, Stanford University, Stanford, California, United States,* [2]*Radiology, Stanford University, Stanford, California, United States,* [3]*Electrical Engineering and Computer Sciences, University of California, Berkeley, California, United States*

PURPOSE: High-resolution volumetric imaging is sensitive to patient motion due to its long scan times. Depending on the k-space sampling trajectory, motion artifacts may appear as ghosting, blurring, and/or additive noise. Given the robustness of Cartesian imaging to off-resonance and other system errors, we focus on ordering the (k_y,k_z)-views in 3D Cartesian imaging. We present a novel method to order and sample the (k_y,k_z) Cartesian grid that is robust to motion effects and ideal for compressed sensing (CS) & parallel imaging (PI). We propose the variable-density radial view-ordering and sampling (VDRad) strategy.

METHOD:

1. *Setup:*
   a. For each view to collect, determine the (k_y,k_z) value: k-space radius, $(k_y^2+k_z^2)^{1/2}$, is adjusted for uneven acceleration and k-space angle, $\arg(k_y+k_z i)$, is adjusted to incorporate a spiral twist.
   b. Given a desired spoke length L_r (each spoke is made up of L_r views), determine the number of spokes necessary to achieve the desired acceleration to form 1 temporal phase.
2. *Ordering:*
   a. Order the samples first by the k-space radius and second by the k-space angle.
   b. Divide the ordered views into L_r rings where the number of points in each ring is proportional to the k-space magnitude (Fig. 1b).
3. *Sampling for each ring:* Using the k-space angle, sample and order each view according to the golden-angle [1,2]: $360°/\varphi \approx 222.5° \Rightarrow 137.5°$ where $\varphi=(1+\sqrt{5})/2$. See Fig. 1c.
4. *Final re-ordering:*
   a. Build spoke *n* by selecting the *n*-th sample in each ring.
   b. For each spoke, the samples can be re-ordered for special considerations. For instance, the samples can be re-ordered for optimal smoothness to minimize eddy current.

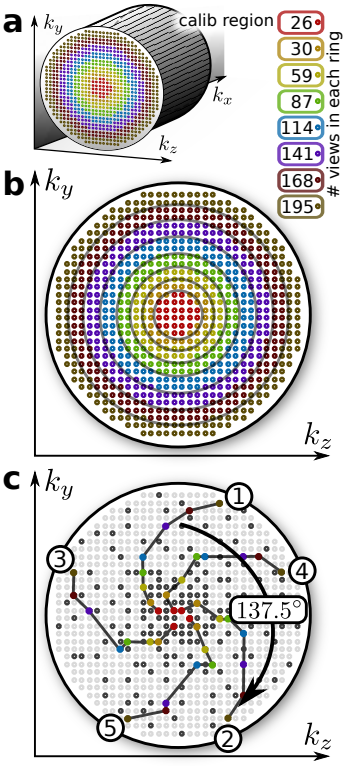

FIG 1 (*left*): *Method overview.* **a:** 3D Cartesian imaging with corner cut. **b:** (k_y,k_z)-views divided into rings. **c:** Sampling/ordering strategy – views are colored according to the corresponding ring; the dark points are sampled after the calibration region is sufficiently covered. Since rings closer to the center have fewer views, these are acquired more rapidly compared to the outer rings. This method generates the variable-density sampling.

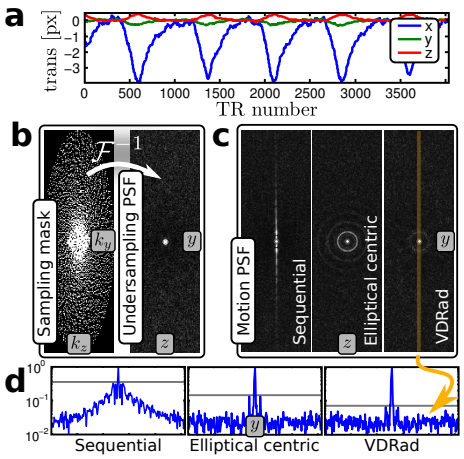

FIG 2: *Sampling pattern analysis.* **a:** Example respiratory motion paths. **b:** Example sampling mask from VDRad using an acceleration factor of 4. **c,d:** Motion effects from view-ordering schemes, modeled as point-spread-functions (PSF). All images have the same window/level. VDRad yields the motion PSF with the smallest side-lobes; VDRad is most effective in localizing artifacts.

EXPERIMENT: All scans were performed on a 3T GE MR750 scanner using a 3D spoiled gradient echo sequence with flip angle = 15° and bandwidth = ±62.5 kHz. Motion was measured using Butterfly navigation [3]. All images were reconstructed using ESPIRiT [4], a CS & PI reconstruction algorithm. In vivo scans were performed free-breathing. See table for specific scan parameters.

	TE/TR [ms]	*Resolution* [mm³]	*FOV* [cm³]	*Navigation time per TR [ms]*	*Coil receiver*	*Acceleration factor*
Phantom	1.7/4.6	1.2×1.2×3.0	30×24×21.6	0.14	30-ch cardiac	8
Abdominal 1	1.4/3.9	1.0×1.3×3.0	34×27.2×18	0.096	32-ch torso	~2.27
Abdominal 2	1.4/3.6	0.88×1.4×2.0	28×22.4×16	0.12	32-ch torso	~3

RESULTS: The single temporal phase reconstruction of the phantom (Fig. 3a) demonstrated that the sampling mask is appropriate for CS & PI. Motion was introduced during the scan (Fig 3b), and a motion-free image (Fig. 3c) was successfully obtained by incorporating data-consistency weights [5] in the ESPIRiT algorithm. Lastly, with VDRad, we were able to reconstruct high-resolution motion-free images from free-breathing scans (Fig. 4) using the weighted ESPIRiT algorithm with motion autofocusing [3].

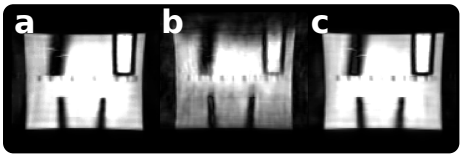

FIG 3: *Phantom study using VDRad.* **a:** Single temporal phase scan. **b:** Ten phases scan with motion. **c:** Data-consistency weights were used to retrospectively soft-gate the acquisition from (b). The sampling/ordering allows for overly corrupt data to be discarded while maintaining an appropriate sampling pattern for CS & PI.

DISCUSSION & CONCLUSION: Our proposed method is an alternative to motion compensated view-ordering, such as ROPE [6] and PAWS [7]. In our method, scan efficiency is partially sacrificed for ease of implementation and robustness to all types of motion. The radial path and golden-angle ordering ensures that k-space is evenly covered even if acquisitions must be discarded. Additionally, for multi-phase imaging, each phase will have a sufficiently different sampling pattern. Lastly, the variable-density sampling ensures an ideal undersampling point-spread-function for CS & PI reconstructions. Some ideal applications for the sampling/ordering include retrospective gating and dynamic contrast enhanced abdominal MRI.

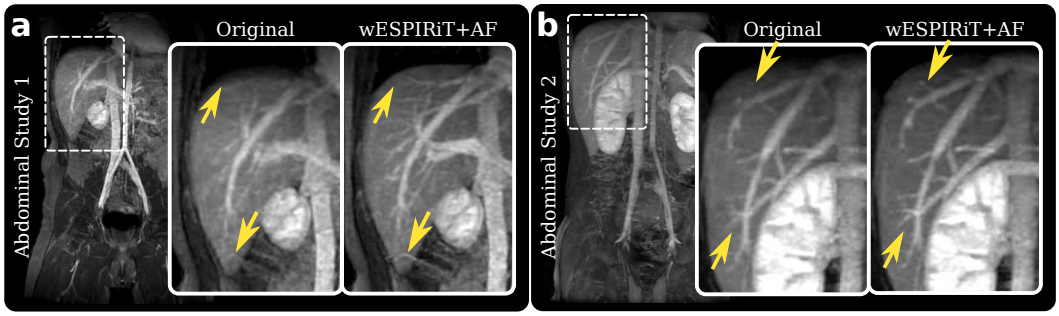

FIG 4: *Abdominal studies using VDRad.* **a:** Post-contrast scan of a 3 year old patient. **b:** Post-contrast scan with fat-saturation of a 5 year old patient. The original images (*left*) are reconstructed using ESPIRiT. Other images (*right*) are reconstructed using weighted ESPIRiT and autofocusing (AF). In these max-intensity-projection images, the large vessels are sharpened and finer vessels are recovered. Diagnostic image quality is obtained despite the free-breathing.

REFERENCES: [1] S Winkelmann et al, IEEETMI 2007; 26:68-76. **[2]** M Doneva et al, ISMRM 2011, p3057. **[3]** JY Cheng et al, MRM 2012; 68:1785-1797. **[4]** M Uecker, P Lai et al, MRM 2012, preprint. **[5]** KM Johnson et al, MRM 2012; 67:1600-1608. **[6]** DR Bailes et al, JCAT 1985; 9:835-838. **[7]** P Jhooti et al, MRM 2000; 43:470-480.